Cellular and Molecular Biology

Journal homepage: www.cellmolbiol.org

Preparation of Nano-microbubbles and Curative Effect of ^{125}I Particles for Primary Liver Cancer Guided by Abdominal Interventional Ultrasound

Yan Chen[#], Shan Gao[#], Yuan Jin, Xiaofeng Wang[*]

Department of B-ultrasound Room of Physical Diagnosis, Daqing Longnan Hospital (The Fifth Affiliated Hospital of Qiqihar Medical College), Daqing, 163453, China

[#]These authors contributed equally to this work as co-first author

ARTICLE INFO

Original paper

Article history:
Received: September 25, 2021
Accepted: March 23, 2022
Published: March 31, 2022

Keywords:
nano-microbubbles, primary liver cancer, contrast-enhanced ultrasound, ^{125}I particles interventional therapy, abdominal interventional ultrasound

ABSTRACT

This study aimed at the preparation of nano-microbubbles (NMBs) and the curative effect of ^{125}I particles for primary liver cancer guided by abdominal interventional ultrasound. NMBs were prepared by the thin-film hydration method, and NMBs and ^{125}I particles were connected by biotin to obtain the NMBs-^{125}I complex.36 patients with primary liver cancer treated in X Hospital from January to December 2019 were selected. NMBs-^{125}I particle implantation was guided by abdominal interventional ultrasound. Computed tomography (CT) or magnetic resonance imaging (MRI) examinations were performed 3 months after treatment, and patients were divided into remission and non-remission groups on account of the results. Contrast-enhanced ultrasound (CEUS) was performed before and 1 month after treatment to analyze and compare the changes in ultrasound parameters. It was shown that there was a good correlation 3 months after treatment between the maximum diameters of the tumor measured by CEUS and CT/MRI, respectively (r=0.856, P<0.01). In the remission group, tRTpre and tTTPprc 1 month after treatment were higher than those before treatment, but tPIpre and tSERmax.pre were lower than those before treatment. In the non-remission group, tRTpre and tTTPprc 1 month after treatment were lower than those before treatment, but tPIpre and tSERmax.pre were higher than those before treatment. Therefore, CEUS had a higher value on the efficacy of the NMBs-^{125}I particle implantation for primary liver cancer.

DOI: http://dx.doi.org/10.14715/cmb/2022.68.3.16

Introduction

Liver cancer is a type of malignant tumor that occurs in the liver, which can be divided into primary and secondary ones. Primary liver cancer accounts for 90% of liver cancers and is one of the common tumors in China. According to the general morphology, it can be divided into massive, nodular and diffuse liver cancers, which are all extremely harmful malignant tumors. Secondary liver cancer is called sarcoma, which is relatively rare compared with primary liver cancer. Secondary or metastatic liver cancer refers to the invasion of the liver by malignant tumors originating from multiple organs throughout the body (1,2). It is more common for liver metastases of malignant tumors from the stomach, biliary tract, pancreas, colorectal, ovary, uterus, lung, breast, and other organs. The incidence of liver cancer is related to drinking alcohol, viral hepatitis, eating moldy food, genetics, and so on. It is often asymptomatic in the early stage, and the liver pain, fever, fatigue, etc. occur in the advanced stage. There is a possibility of cure in the early stage, and the middle-stage treatment is more complicated (3,4). In China, liver cancer is a malignant tumor with high morbidity and mortality among men under 60, having a serious impact on patients and their families. Laboratory examinations of liver cancer show the elevated alpha-fetoprotein (AFP) and the hemagglutination >1:100, which can be considered as a possibility of liver cancer. Auxiliary examinations include contrast computerized tomography (CT) and magnetic resonance imaging (MRI), as liver cancer is mainly manifested as early tumor contrast enhancement, and multiple blood vessels, tumor blood vessels, or arteriovenous communication can be observed in more than 90% of the hepatic arteriography (5).

With the continuous development of science and technology, radiotherapy for liver cancer is also developed constantly. There are many ways for radiotherapy in the clinic. The best radiotherapy is to

*Corresponding author. E-mail: lujiaonuo4924@163.com

irradiate the target lesion only without causing radiation damage to the lesion. However, the liver is a radiation-sensitive organ, and the incidence of radioactive liver injury will increase as the radiation dose exceeds 40Gy. How to use the required dose during radiotherapy without damaging stem cells has been a difficult issue in radiotherapy (6,7). Some researchers implanted ^{125}I into the transplanted tumors of liver cancer, and the degeneration and necrosis of tumor cells were detected 21 days after the implantation. For patients with advanced liver cancer, the control rate can reach 87% after ^{125}I treatment, and the life quality of patients would be greatly improved (8,9). In the screening of liver diseases, ultrasound is the preferred method as it's convenient, safe, and low-cost. Contrast-enhanced ultrasound (CEUS) can improve the quality of the image and reflect the blood supply inside the tumor. Quantitative ultrasound analysis of liver cancer is more and more applied in its early screening, and it is also possible to map the region of interest of tumors.

Adding nano-microbubbles (NMBs) to the ultrasound contrast agent is an effective means to realize the drug loading capacity of the contrast agent. Ultrasound contrast agents can enhance the acoustic contrast, and it has tended to develop in the direction of nano-level and functionalization. Studies have shown that NMBs contrast agent combined with ultrasound technology can make localized drug release by continuous ultrasound and pulsed ultrasound (10). As a drug carrier, CEUS has a low drug loading capacity and large particle size, which limits its operation to the tumor target organs and tissues to release drugs. NMBs can help the release of drugs. CEUS can be in the form of soft thin-film microbubbles that wrap high-density inert gas. Compared with conventional angiography, CEUS has a strong penetrating power; and NMBs with a particle size as small as 500nm can produce an effective contrast effect at 7.5Hz, thereby the drug loading of ultrasound contrast can be realized (11,12). Polyglycolic acid, polylactic acid (PLA), and their copolymer have good biocompatibility, stability, and modifiability, and are widely used in biodegradable medical materials. NMBs are unstable as being prepared with PLA alone, and microbubble shells need to be added to enhance drug compatibility. Lecithin has good fluidity and flexibility, and it can be completely absorbed by the human body without any toxicity. Poly lactic-co-glycolic acid (PLGA) copolymer nanospheres are widely used as drug carriers in radiotherapy due to their good biocompatibility, slow-release property, and large drug loading capacity (13,14).

In this study, the combination of lecithin and PLA was used as the shell material of the NMBs, and the modified ultrasonic multiple emulsions were used to prepare the NMBs-^{125}I complex. The therapeutic effect of the ^{125}I particles on patients with primary liver cancer was discussed, while the PLA-lecithin NMBs-^{125}I particles were injected by the CEUS. This study offered an effective basis for the treatment of cancer patients clinically.

Materials and methods

Clinical data

36 patients with liver cancer were selected for this study and were treated in X Hospital from January to December 2019. The implantation of the NMBs-^{125}I complex was guided by abdominal interventional ultrasound. CT or MRI was performed 3 months after treatment. The patients were divided into the remission group (n=18) and the non-remission group (n=18) based on the examination results, and they were all diagnosed with primary liver cancer through the clinical diagnosis or cytological examination. Among the 18 cases in the remission group, 8 were males and 10 were females. They were aged 38-68 (62.46±6.9) years old with a weight of 58-81 (70.1±9.1) kg. For the Child-push grading of their liver functions, 11 cases were confirmed in grade A, and 17 cases were in grade B. With the Barcelona clinic liver cancer (BCLC) staging, 7, 2, and 1 case were diagnosed in stage B, stage C, and stage D, respectively. 13 cases were males and 15 were females in the non-remission group, and they were 39-67 (63.06±6.9) years old with the weight of 57-81 (72.3±8.6) kg. According to their BCLC staging, 10, 7, and 1 cases were determined to be in stage B, stage C, and stage D, respectively. With the Child-push grading of liver functions, 13 cases were included in grade A and 5 cases were in grade B. No pleural effusion or ascites and no distant metastasis were found before surgery, which was in line with the indications for the treatment of primary liver cancer with local ^{125}I radioactive particles. Patients

complicated with metabolic diseases and hematological diseases were excluded. There was no statistically significant difference in the general data of the included patients. All the patients and their families signed informed consent of this study, which were reviewed and approved by the Medical Ethics Committee of X Hospital.

The inclusion criteria were described as follows. Patients with primary liver cancer received ^{125}I radioactive particle implantation in the department of interventional ultrasound in X Hospital. All patients tolerate local anesthesia, and the maximum diameter of the lesion didn't exceed 5cm. Before treatment, the target lesion had not received any tumor-related treatment. The survival time of patients was greater than 6 months.

The exclusion criteria below were followed. Patients were in the acute inflammatory phase, or they had severe mental and cardiovascular diseases. Excessive breathing was found during the radiography, together with a poor contrast imaging display of the target lesions, which can't meet the quantitative analysis. Patients had severe disturbance of consciousness or intractable ascites. Patients were allergic to sulfur hexafluoride or other constituents.

Equipment and materials

The ^{125}I particles produced by Shanghai Xinke Pharmaceutical Co., Ltd. were chosen, with the approval number of H200413506711/BT-125I of the State Food and Drug Administration. 18G particle implantation needles and gun-type implanters were used for the particle implantation. The Sequoia512 ultrasound machine was made by Acuson Corporation in Mountain View, California of SiemensLtd., with the contrast software and 4V1 probes (3.0-4.5MHz).

The particle tissue penetration was 1.7cm, the initial dose rate was 7cGy/h, the half-life period was 59.6d, and the radioactivity was 0.8mCi. The GR-3000 radioactive particle treatment planning system of Zhuhai Hokai Medical Instruments Co., Ltd. was adopted for the computer treatment planning.

Therapeutic methods

All patients who received radioactive particle implantation to treat liver cancer hadn't undergone radiotherapy, transhepatic arterial chemotherapy and embolization, liver cancer surgery, and other related treatments before. All the included patients needed to have an ultrasound examination (CT or MRI) to obtain the image of lesions before surgery (0-3 days before particle implantation). All patients were treated with ^{125}I particles interventional therapy, with the ultrasound-mediated PLA-lecithin NMBs injection. The images were input to the treatment planning system to calculate the required number, spatial distribution, and dose of particles. The radioactivity of the implanted NMBs-^{125}I particles was 0.8mCi, and ultrasound gave the real-time guided images. Before the surgery, disinfection and the surgical drape were required. After local infiltration anesthesia, the direction and depth of the guide needle were adjusted according to the ultrasound-guided images. The principle of implanting particles was, that they should be densely implanted on the periphery and sparsely implanted in the middle. 18G implantation needle entered the liver through the selected puncture point on the skin, and the needle core was taken out when the needle was 1.0-1.5cm away from the distal edge of the target tumor. The particle was sent into the needle through the needle core, and the gun-type implanter was removed. The needle core was pushed to send the particle into the liver tumor, and then the needle core was retracted from far to near according to the set distance. The next particle was implanted according to the calculation until all the particles at this position were implanted. For tumors with a diameter greater than 3.5cm, 2-4 insertion points were selected, and the vertical and horizontal spacing of each particle was 1.0-1.5cm. When the diameter of the tumor was less than 3.5cm, 1-2 insertion points were chosen, and the vertical and horizontal spacing in particles was also 1.0-1.5cm. The patients in the observation group completed the ultrasound-guided NMBs-^{125}I particles implantation treatment successfully.

Follow-up after surgery was to know the survival conditions, clinical symptoms, and related complications of patients in time; regular liver function reexamination was required. CEUS examination was performed before the treatment and 1 month after surgery, respectively, to analyze and compare the ultrasound parameters in the two periods. 1 and 3 months after treatment, the tumors were measured by CEUS and CT/MRI, and the obtained maximum diameters under two methods were used for

the correlation analysis between the examination methods.

Preparation of microbubble ultrasound contrast agent

The blank PLA-lecithin NMBs ultrasound contrast agent was prepared by the ultrasonic multiple emulsion-solvent volatilization method. First, 1mL 0.01g/mL sodium formate ($NaHCO_2$) solution was added to 10mLdichloromethane (CH_2CI_2) with PLA and lecithin with different ratios (oil phase), to prepare the water phase (W1). They reacted under 200W ultrasonic wave for 100s, then the water-in-oil (W1/O) primary emulsion was formed. The primary emulsion was injected into 0.01g/mL poloxamer solution with 1% Tween-80 (W2, external water phase), and then the water-in-oil-in-water (W1/O/W2) multiple emulsion was generated. The multiple emulsions were slowly stirred for 10 hours to make the organic solvent volatilize, centrifuged at 8000r/min and washed twice. The precipitation was collected, 2mL 0.05g/mL mannitol was added, and the mixture was lyophilized. The paclitaxel was in 3mg/mL. During the preparation of NMBs, the fluorescent dyes Rhodamine B and paclitaxel could be added to the organic phase.

Characterization of drug-loaded NMBs

X-ray powder crystal diffraction technique was adopted to detect the form of the drug in NMBs while scanning connection and transmission electron microscopy were used to detect the internal and external morphology of NMBs. The laser scanning confocal technique was applied to detect the PLA-lecithin NMBs containing Rhodamine B, and the particle size was measured via a nanoparticle Zeta potential analyzer after the NMBs were dispersed in water.

Determination of drug loading capacity and encapsulation efficiency of NMBs

The high-performance liquid chromatography was applied, with a column temperature was 25℃, and a wavelength was 227nm. The chromatographic column was Symmetry C18 stainless steel column, with a specification of (250mm×4.6mm, 5μm). The volume ratio of mobile phase methanol to water was expressed to be V (methanol):(Water) =75:25; and the flow velocity was 1.0mL/min. For the precisely prepared methanol standard solution of 1-1μg/mL with paclitaxel, the injection volume was fixed as 15μL, and the X-axis and Y-axis of the standard curve represented the volume concentration of the standard solution and the peak area, respectively. 10mg lyophilized powder and 0.5mL CH_2CI_2 were placed in a centrifuge tube. After the NMBs were dissolved ultrasonically, 2.5mL methanol (CH_3OH) was added for swirling for 10 minutes, then centrifuged at 8000r/min for 10 minutes. 15μL supernatant was taken. The measured peak area was substituted into the standard curve, then the concentration of paclitaxel was worked out. Encapsulation efficiency and drug loading capacity were calculated according to the following equation [1].

$$DC=\frac{M1}{M2}\times 100\% \quad [1]$$

M1 represented the mass of paclitaxel; M2 represented the mass of NMBs.

$$EF=\frac{W1}{W2}\times 100\% \quad [2]$$

In equation [2], *W1* and *W2* were the actual and the theoretical drug loading capacity, respectively.

The tumor inhibition rate was obtained by equation [3] below.

$$IR=1-\frac{E1}{E2}\times 100\% \quad [3]$$

E1 was the weight of patients in the observation group, and *E2* was the average tumor mass of the patients in the control group.

Statistical methods

SPSS 22.0 was used for data analysis. The enumeration data were expressed as [cases (%)], and the comparison between two groups was performed by χ^2 test. Pearson correlation analysis was adopted to detect the correlation between the maximum diameters of the tumor measured by CEUS and CT/MRI. The difference was statistically significant with $P<0.05$.

Results and discussion

Scanning electron microscope images of NMBs with different lecithin contents

From the electron micrographs of the NMBs in Figure 1, it was observed that the lecithin content had some effect on the morphology of the NMBs. In Figure 1, Figure A was the image without lecithin and

Figures B and C were the electron micrographs with lecithin. With the increase of lecithin content, the NMBs were easier to disperse and the redissolution process speeded up. In Figure 1B, the mass ratio of PLA to lecithin was 250:50. In Figure 1C, when the lecithin content increased to 100%, the NMBs disappeared and only nanoparticles were presented.

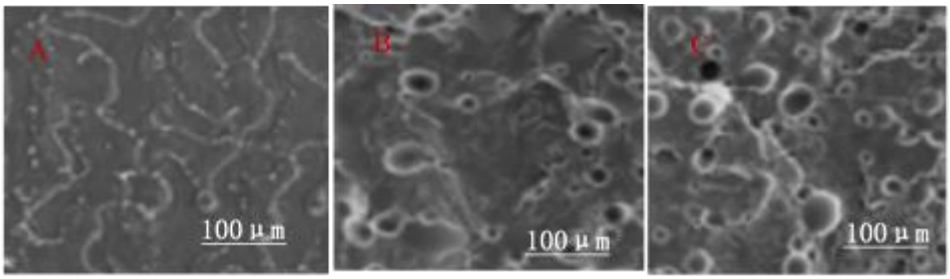

Figure 1. Electron microscope images of NMBs with different lecithin contents.

Effect of lecithin content changes on NMBs

The effect of different lecithin contents on the particle size distribution was shown in Figure 2. As the lecithin content increased, the particle size of the NMBs decreased, and the particle size dispersibility also decreased. The NMBs with a ratio of the two between 100:200 and 150:150 tended to be stable, showing that lecithin stabilized NMBs.

PLA-lecithin NMBs

Figure 3 showed the images of PLA-lecithin NMBs. Images A and B were the electron microscope images of NMBs, while image C was the laser scanning confocal microscope image. It was found that the NMBs were broken, showing that the NMBs were in a hollow structure. The laser scanning confocal image showed that there was a hollow structure of NMBs in the carrier layer of Rhodamine as well. Image D was the original image of NMBs under the microscope.

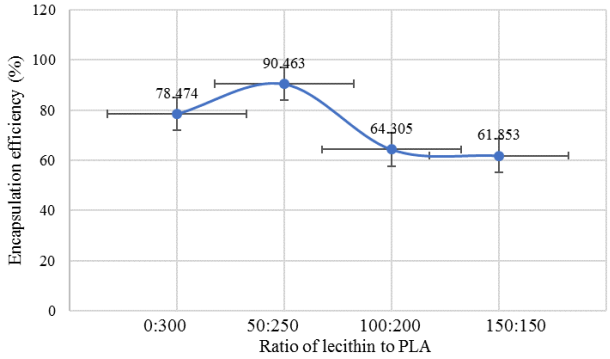

Figure 2. Effect of different lecithin contents on particle size distribution.

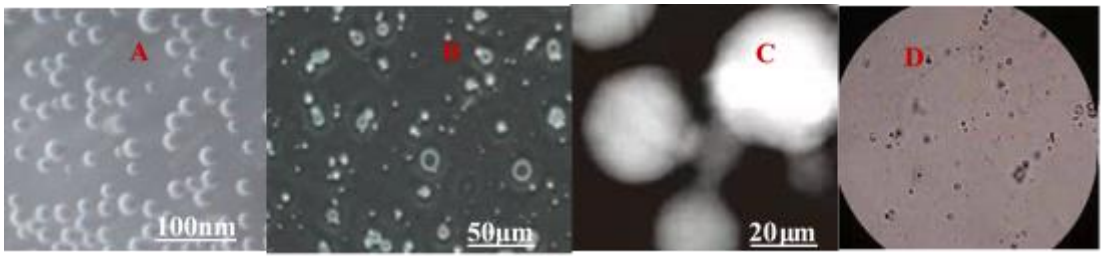

Figure 3. PLA-lecithin NMBs.

Drug releasing curve of microspheres in vitro

It was shown in Figure 4 that the drug was released after being acted by the ultrasound machine. Ultrasound had the effect of promoting the drug release and the characteristic of targeted drug-loaded particles.

Comparison of the patient's images

Figure 5 showed the images of a 57-year-old male patient with primary liver cancer. He had no symptoms of obvious upper abdominal pain, nausea and vomiting, and thoracic oppression and shortness of breath. The examination in the hospital showed the

giant space-occupying lesion in his liver. After treatment, lipiodol was deposited in a mass in the right lobe and chronic inflammation occurred in the maxillary sinus of the left lobe. The image on the right showed that, 6 months after treatment, the tumor was significantly smaller than that before.

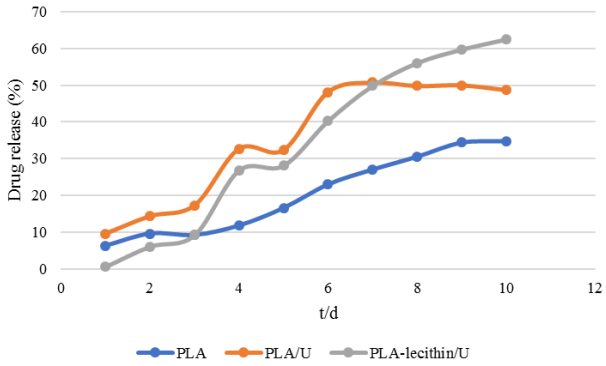

Figure 4. In vitro drug release curves of microspheres.

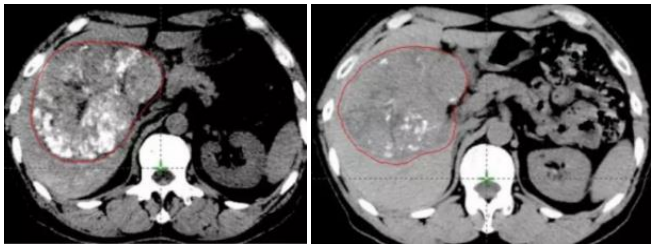

Figure 5. Medical images of a patient.

Comparison of the maximum diameters of the tumor measured by CEUS and CT/MRI

As shown in Figure 6, 3 months after treatment, there was a good correlation between the maximum diameters of the tumor measured by CEUS and CT/MRI (r=0.856; P<0.01).

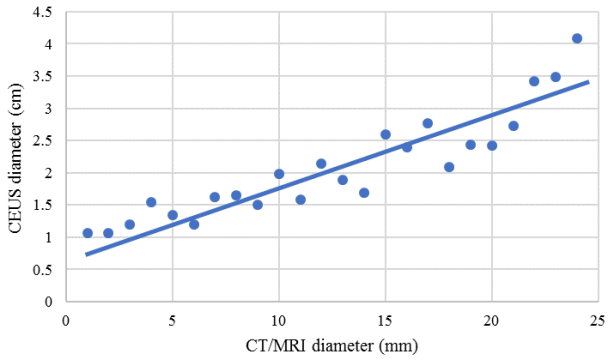

Figure 6. The maximum diameters of the tumor were measured by CEUS and CT/MRI.

Changes in CEUS quantitative parameters

The rise time (RT), time to peak (TTP), peak intensity (PI), and maximum time slot enhancement ratio (TSermax) were compared. As shown in Figure 7, in the remission group, tRTpre and tTTPprc 1 month after treatment were higher than those before treatment, but tPIpre and TSermax.pre were lower than those before treatment.

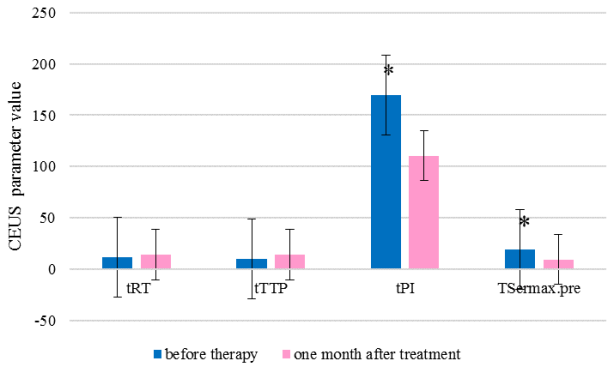

Figure 7. Comparison of CEUS parameters in the remission group before and one month after treatment. (* indicated the statistically significant differences as P<0.05.)

In Figure 8, in the non-remission group, tRTpre and tTTPprc 1 month after treatment were lower than those before treatment, but tPIpre and TSermax.pre were higher than those before treatment.

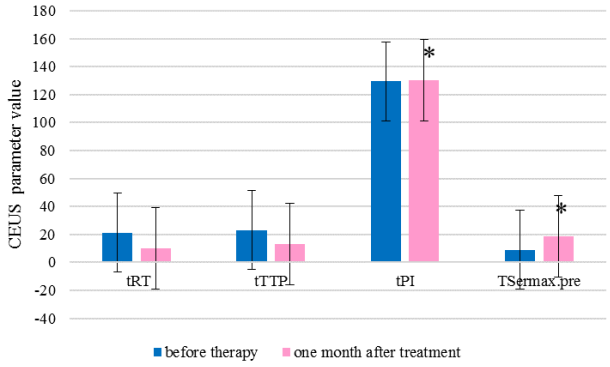

Figure 8. Comparison of CEUS parameters in the non-remission group before and one month after treatment. (* indicated there was a statistically significant difference as P<0.05.)

Comparison of adverse reactions and tumor inhibition rates between the two groups

The incidence of adverse reactions and tumor inhibition rates were compared between the two groups. It was suggested that the tumor inhibition rate

of patients in the observation group 6 months after treatment was significantly higher than that of the control group (75.67% vs 13.43%). The incidence of adverse reactions in patients in the observation group was also much lower than that of the control group (5.76% vs 29.87%) (P<0.05) (Figure 9).

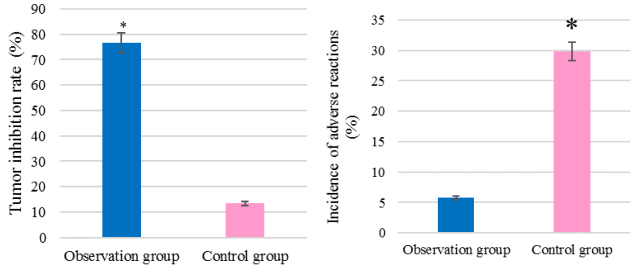

Figure 9. Comparison of the incidence of adverse reactions and tumor inhibition rates between two groups. Note: * marked the statistically significant differences compared to the observation group (P<0.05).

Ultrasound contrast agents can enhance the contrast of ultrasound imaging and are useful for the detection and imaging of microvascular perfusion in clinical practice. Many conventional angiographies can't locate the tissue structure caused by diseases well, and the accuracy of the diagnosis of soft tissue damage isn't high, leading to misdiagnosis and missed diagnosis (15,16). The ideal ultrasound contrast agent can flow throughout the body with the blood and can reflect the blood perfusion of the organs accurately. Meanwhile, it won't affect the blood flow of the body, with an appropriate half-life period, appropriate size, good dispersibility, and no toxicity (17). Ultrasound microbubbles can change the scattering and attenuation of ultrasound by tissues and organs, and enhance the image signal by changing the propagation speed of ultrasound in the tissues, thereby improving the specificity and sensitivity of diagnosis (18,19). The researches of ultrasound microbubble combined with ultrasound radiation on tumors is mainly to encapsulate and transfer the drug to the tumor site through the drug delivery system. After the ultrasound, cavitation and rupture occur in the microbubbles, and the drug is released. It can reduce the drug accumulation in other organs, increase the drug accumulation in the cells, and reduce toxicity (20). Liver cancer is a common malignant tumor. Radioactive particle implantation is a new method for the treatment of liver cancer, and ^{125}I particle implantation offers a new way the treatment with metastasis, recurrence, and refractoriness (21). Song et al. (2021) (22) adopted ^{125}I particle implantation therapy for patients who underwent hepatic artery chemoembolization, and ^{125}I particle implantation and intertumoral injection gave good effects on hepatocellular cancer. Zhou et al. (2021) (23) treated patients with locally advanced pancreatic head cancer using ^{125}I particle implantation, which improved the biochemical indicators and relieve the pain of patients effectively with fewer complications.

With the continuous development of ultrasound molecular imaging technology and biotechnology, ultrasound contrast agents have gradually developed from the micron level to the nano level. The particles of NMBs have the stronger penetrating power, to penetrate the capillaries of tumor tissues and inject them into the tumor. NMBs can accelerate the drug release with the interventional ultrasound, having a good drug effect (24, 25). Oeffinger and Wheatley (2004) (26) studied that the NMBs had an enhanced effect on ultrasound contrast. After the substance reaches the nano-level, the characteristics of molecular structure would change greatly; which showed a new idea for the application of nano-level contrast agents medically. Ultrasound contrast agents present the advantages of high targeting, high efficiency, and miniaturization. It should be noted that by inorganic and organic nanomaterials, various medical applications are possible (27-30). In this study, PLA-lecithin NMBs with good dispersibility were prepared. The encapsulation efficiency of NMBs reached (91.24±5.49) %, and the drug loading capacity was (8.81±0.63) %, showing great results.

Conclusions

In summary, the PLA-lecithin NMBs-^{125}I particles injection guided by CEUS was researched in this study, and a good effect was shown on the treatment of patients with primary liver cancer. The ^{125}I particles were distributed in the shell of NMBs in an amorphous state, and the in vitro drug release of the NMBs had the characteristics of slow-release, zero-order release, and accelerated drug release with interventional ultrasound. The clinical study suggested that the ultrasound-mediated PLA-lecithin NMBs-^{125}I particles injection could reduce the toxicity and side effects of drugs, and increase the tumor inhibition rate, with a high application value clinically. The

nano-ultrasound contrast agent was proposed in this study, which provided a new way for tumor research. The drugs with extremely high purity and good medicinal properties were obtained using the NMBs preparation technology. It is believed that with the development of nanotechnology, nano-suspension drug delivery technology will achieve more.

The sample size was relatively small, which was the disadvantage of this study. The NMBs needed to be studied from more perspectives, such as infrared rays. The small sample size also brought a certain impact on the research results; therefore, the expanded sample size was needed for further study.

Acknowledgments

Not applicable.

Conflict interest

The authors declare that they have no conflict of interest.

References

1. Kim D, Lee JH, Moon H, Seo M, Han H, Yoo H, Seo H, Lee J, Hong S, Kim P, Lee HJ, Chung JW, Kim H. Development and evaluation of an ultrasound-triggered microbubble combined transarterial chemoembolization (TACE) formulation on rabbit VX2 liver cancer model. Theranostics 2021; 11(1):79-92.
2. Wu J, Sun L, Liu T, Dong G. Ultrasound-Targeted Microbubble Destruction-Mediated Downregulation of EZH2 Inhibits Stemness and Epithelial-Mesenchymal Transition of Liver Cancer Stem Cells. Onco Targets Ther 2021;14:221-237.
3. Sun M, Shang P, Bai J, Li S, Li M. High-intensity focused ultrasound ablation combined with transcatheter arterial chemoembolization improves long-term efficacy and prognosis of primary liver cancer. J Clin Lab Anal 2021;35(2):e23633.
4. Hijioka S, Okusaka T. Enormous Potential of Endoscopic Ultrasound-guided Liver Biopsies. Intern Med 2021;60(11):1655-1656.
5. Petta S, Sebastiani G, Viganò M, Ampuero J, Wai-Sun Wong V, Boursier J, Berzigotti A, Bugianesi E, Fracanzani AL, Cammà C, Enea M, Grottes MD, Di Marco V, Younes R, Keyrouz A, Mazzola S, Mendoza Y, Pennisi G, Romero-Gomez M, Craxì A, de Ledinghen V. Monitoring Occurrence of Liver-Related Events and Survival by Transient Elastography in Patients With Nonalcoholic Fatty Liver Disease and Compensated Advanced Chronic Liver Disease. Clin Gastroenterol Hepatol 2021;19(4):806-815.e5.
6. Li J, Yu T, Zhang L, Yang M, Gao S, Pu N, Li C, Wang C, Gong G, Cheng J, Wang L, Li G, Wang X, Chen Y. An iodine-125 seed strand combined with a metal stent versus a metal stent alone for obstructive jaundice caused by pancreatic ductal adenocarcinoma. Brachytherapy 2021;20(2):446-453.
7. Li CG, Zhou ZP, Jia YZ, Tan XL, Song YY. Radioactive 125I seed implantation for pancreatic cancer with unexpected liver metastasis: A preliminary experience with 26 patients. World J Clin Cases 2021;9(4):792-800.
8. Xu Y, Du J, Wang Y, Gong B, Wang Y, Qian L, Tan Y. A Highly Responsive Pancreatic Ductal Adenocarcinoma with Liver Metastasis: A Rare Case Report. Int J Gen Med 2021;14:487-496.
9. Yang M, Yan Z, Luo J, Liu Q, Zhang W, Ma J, Zhang Z, Yu T, Zhao Q, Liu L. A pilot study of intraluminal brachytherapy using 125I seed strand for locally advanced pancreatic ductal adenocarcinoma with obstructive jaundice. Brachytherapy 2016;15(6):859-864.
10. Jin Z, Chang J, Dou P, Jin S, Jiao M, Tang H, Jiang W, Ren W, Zheng S. Tumor Targeted Multifunctional Magnetic Nanobubbles for MR/US Dual Imaging and Focused Ultrasound Triggered Drug Delivery. Front Bioeng Biotechnol 2020;8:586874.
11. Xie F, Zhang D, Cheng L, Yu L, Yang L, Tong F, Liu H, Wang S, Wang S. Intradermal microbubbles and contrast-enhanced ultrasound (CEUS) is a feasible approach for sentinel lymph node identification in early-stage breast cancer. World J Surg Oncol 2015;13:319.
12. Zhang C, Li Y, Ma X, He W, Liu C, Liu Z. Functional micro/nanobubbles for ultrasound medicine and visualizable guidance. Sci China Chem 2021:1-16.
13. Cavalcante RS, Ishikawa U, Silva ES, Silva-Júnior AA, Araújo AA, Cruz LJ, Chan AB, de Araújo Júnior RF. STAT3/NF-κB signalling disruption in M2 tumour-associated macrophages is a major target of PLGA nanocarriers/PD-L1 antibody immunomodulatory therapy in breast cancer. Br J Pharmacol 2021;178(11):2284-2304.
14. Bakhaidar R, O'Neill S, Ramtoola Z. PLGA-PEG Nanoparticles Show Minimal Risks of Interference with Platelet Function of Human Platelet-Rich Plasma. Int J Mol Sci 2020;21(24):9716.

15. Jafari Sojahrood A, de Leon AC, Lee R, Cooley M, Abenojar EC, Kolios MC, Exner AA. Toward Precisely Controllable Acoustic Response of Shell-Stabilized Nanobubbles: High Yield and Narrow Dispersity. ACS Nano 2021;15(3):4901-4915.
16. Vidallon MLP, Tabor RF, Bishop AI, Teo BM. Ultrasound-assisted fabrication of acoustically active, erythrocyte membrane "bubbles". Ultrason Sonochem 2021;72:105429.
17. Wang Y, De Leon AC, Perera R, Abenojar E, Gopalakrishnan R, Basilion JP, Wang X, Exner AA. Molecular imaging of orthotopic prostate cancer with nanobubble ultrasound contrast agents targeted to PSMA. Sci Rep 2021;11(1):4726.
18. Geyer T, Rübenthaler J, Froelich MF, Sabel L, Marschner C, Schwarze V, Clevert DA. Contrast-Enhanced Ultrasound for Assessing Abdominal Conditions in Pregnancy. Medicina (Kaunas) 2020;56(12):675.
19. Schwarze V, Rübenthaler J, Čečatka S, Marschner C, Froelich MF, Sabel BO, Staehler M, Knösel T, Geyer T, Clevert DA. Contrast-Enhanced Ultrasound (CEUS) for the Evaluation of Bosniak III Complex Renal Cystic Lesions-A 10-Year Specialized European Single-Center Experience with Histopathological Validation. Medicina (Kaunas) 2020;56(12):692.
20. Kloth C, Kratzer W, Schmidberger J, Beer M, Clevert DA, Graeter T. Ultrasound 2020 - Diagnostics & Therapy: On the Way to Multimodal Ultrasound: Contrast-Enhanced Ultrasound (CEUS), Microvascular Doppler Techniques, Fusion Imaging, Sonoelastography, Interventional Sonography. Rofo 2021;193(1):23-32.
21. Wang HW, Li XJ, Li SJ, Lu JR, He DF. Biliary stent combined with iodine-125 seed strand implantation in malignant obstructive jaundice. World J Clin Cases 2021;9(4):801-811.
22. Song Z, Guo X, Yin C, Wang Y. Therapeutic efficacy of TACE 125I seed implantation and its combination with intra-tumor injection of cisplatin for the treatment of hepatocellular carcinoma. Indian J Cancer 2021;58(1):57-61.
23. Zhou S, Zhu C, Chen SL, Li JA, Qu KL, Jing H, Wang Y, Pang Q, Liu HC. 125I Intracavitary Irradiation Combined with 125I Seeds Implantation for Treatment of Locally Advanced Pancreatic Head Cancer: A Retrospective Analysis of 67 Cases. Int J Gen Med 2021;14:2645-2653.
24. Lanza GM, Wickline SA. Targeted ultrasonic contrast agents for molecular imaging and therapy. Curr Probl Cardiol 2003;28(12):625-53.
25. Exner AA, Kolios MC. Bursting Microbubbles: How Nanobubble Contrast Agents Can Enable the Future of Medical Ultrasound Molecular Imaging and Image-Guided Therapy. Curr Opin Colloid Interface Sci 2021;54:101463.
26. Oeffinger BE, Wheatley MA. Development and characterization of a nano-scale contrast agent. Ultrasonics 2004;42(1-9):343-7.
27. Alavi M, Adulrahman NA, Haleem AA, Al-Râwanduzi ADH, Khusro A, Abdelgawad MA, Ghoneim MM, Batiha GES, Kahrizi D, Martinez F, Koirala N. Nanoformulations of curcumin and quercetin with silver nanoparticles for inactivation of bacteria. Cellular and Molecular Biology 2022;67(5):151–156.
28. Chen Y, Chen SJ, Li S, Wei JJ. SERS and DFT study of p-hydroxybenzoic acid adsorbed on colloidal silver particles. Cellular and Molecular Biology 2015;61(5), 11–15.
29. Khaledian S, Kahrizi D, Moradi S, Martinez F. An experimental and computational study to evaluation of chitosan/gum tragacanth coated-natural lipid-based nanocarriers for sunitinib delivery. J Mol Liq 2021 Jul 15;334:116075. doi: 10.1016/j.molliq.2021.116075.
30. Zaki EI, El-Seedy AS, Kelada IP, Sharafeldin NA, Mouaty HM, Ramadan HS. Impact of citrate-and chitosan-capped gold nanoparticles on the liver of Swiss albino mice: Histological and cyto-genotoxic study. Cell Mol Biol 2019;65(5).